Tracing Carbon Flow to Unravel Carbon Lock-In in China through a Supernetwork-Based Perspective for Targeted Decarbonization

Abstract

The pathway to carbon neutrality requires not only reducing emissions but also addressing the structural complexity of how emissions are generated, transmitted, and embedded across regions and sectors. Conventional mitigation strategies target high-emission locations, yet they overlook who emits, who enables, and who intermediates in the carbon system. This study develops a carbon flow supernetwork by integrating multi-regional input-output analysis with supernetwork theory, enabling tracing where emissions occur, how they move, and who sustains them from 2007 to 2017. Results reveal a three-layered structure of carbon lock-in in China. Upstream emitters like Inner Mongolia, Shanxi, and Hebei concentrate emissions through coal-based electricity and heavy industries. Downstream distributors, notably coastal regions such as Guangdong and Jiangsu, account for over 60% of carbon inflows via embedded trade and final demand. Structural intermediaries, including Shandong and Henan via logistics and information services, exhibit high network centrality and govern carbon circulation despite moderate emission levels. Furthermore, the Jing-Jin-Ji and Yangtze River Delta function as systemic carbon anchors, where dense industrial networks and embedded supply chains lock China's economy into high-emission trajectories. As the system matured from 2007 to 2015, connectivity and internal carbon cycling increased, but signs of topological reconfiguration emerged post-2015, coinciding with China's green transition efforts. Carbon governance should shift from targeting emission volume to incorporating network-sensitive, system-level interventions. Prioritizing central intermediaries and redesigning flow pathways offers a more effective and equitable route toward carbon neutrality in structurally complex economies like China.

Keywords: Carbon lock-in; Supernetwork; Multi-regional input-output; Carbon flow

1 Introduction

Climate change, driven largely by anthropogenic carbon emissions, has become one of the most pressing global challenges [1]. International frameworks such as the Kyoto Protocol and the Paris Agreement aim to mitigate this crisis [2]. As the world's largest carbon emitter, China plays a pivotal role in global climate governance [3]. At the 2020 UN General Assembly and Climate Ambition Summit, China announced ambitious dual carbon goals: peaking emissions before 2030 and achieving carbon neutrality by 2060 [4-6]. To fulfill these objectives, China faces the critical task of balancing economic growth, regional equity, and environmental sustainability, which requires exploring differentiated low-carbon development pathways tailored to regional resource endowments and industrial structures [7,8].

However, after decades of rapid industrialization, China's economic system faces significant challenges due to entrenched path dependencies and carbon lock-in, characterized by continued investment in carbon-intensive industries and technologies [9]. The concept of carbon lock-in, foundationally developed by Unruh [10,11], highlights how technological, institutional, and infrastructural inertia reinforce high-carbon pathways. This perspective can capture structural persistence in carbon flows, noting that unlike carbon or energy dependency, lock-in stresses systemic entrenchment rather than reliance on specific inputs [12,13]. Regional disparities in resource distribution and development stages intensify conflicts between emission reduction responsibilities and regional equity [14]. Yet these disparities are not isolated: economically developed coastal regions, driven by advanced manufacturing and trade, are tightly linked with resource-rich inland provinces through embodied carbon flows, outsourcing high-carbon production while relying on upstream energy and materials [15]. Such interregional linkages exacerbate regional inequalities and amplify the difficulty of allocating emission responsibilities in an equitable manner [16,17]. From an industrial perspective, entrenched high-carbon technologies and traditional industrial structures form another barrier to low-carbon transformation [18,19]. Resource-dependent industries, such as power generation and construction, have historically dominated China's economic growth model [20], embedding regions in dual lock-in scenarios of high-carbon and low-value production pathways [21]. These sectoral lock-ins are further reinforced through cross-sectoral couplings—for example, electricity and coal supplying carbon-intensive inputs to downstream construction—making industrial adjustment a systemic rather than sector-specific challenge. Transitioning away from these pathways therefore requires not only balancing emission mitigation and regional development priorities, but also designing coordinated governance mechanisms that explicitly target the cross-regional and cross-sectoral interactions underpinning China's carbon flow system.[22,23]. Nevertheless, mitigation policy designs have often emphasized short-term localized targets, lacking the coordination needed for coherent long-term carbon governance across regions and sectors [24,25].

To effectively understand and address these complex challenges, comprehensive approaches are necessary. Scholars have increasingly turned to Multi-Regional Input-Output (MRIO) analysis as a powerful tool to map the flow of embodied emissions across regions and sectors [26-29]. MRIO models capture how consumption in one region induces emissions elsewhere through interlinked supply chains [30,31], thus enabling the identification of environmental responsibilities across regions and sectors [32-34]. In China's context, MRIO-based studies have revealed the extensive transfer of carbon emissions from economically advanced eastern provinces to less-developed central and western regions [35,36]. Internationally, extensions of MRIO methods such as structural decomposition analysis and environmental input-output network models have provided insights into how trade, industrial structure, and final consumption shape global and bilateral carbon emissions [37-40]. While MRIO models quantify carbon flows, they are often limited in explaining the structural mechanics of these flows [41]. Specifically, MRIO analyses focus on volume-based attribution but lack tools to investigate the network logic—i.e., who emits, who enables, and who intermediates—within complex carbon systems. Addressing this limitation requires methodological integration with advanced network science. Supernetwork theory, which models interdependent, multi-layered networks, offers a promising framework to capture the structural intricacies of regional-sectoral carbon interactions [42]. Emerging applications of supernetwork methodologies, such as variational inequalities [43], hypergraphs [44], and network-based models [45], have proven effective in fields including supply chain management, transportation systems, and information diffusion [46-51]. However, their application to carbon emissions, especially regarding detailed structural characteristics such as node interactions and network topology at the regional-sectoral scale, remains scarce [52,53].

To fill this gap, we extend the analytical focus from emission magnitudes to the structural mechanisms that sustain high-carbon trajectories. Here, carbon lock-in is operationally defined as a systemic form of high-carbon path dependence embedded in regional-sectoral interaction structures, rather than mere technological or resource dependence. It emphasizes how interlinked regions and sectors collectively reinforce carbon-intensive development pathways. Building on this conceptualization, this study proposes a carbon flow supernetwork framework that integrates MRIO modeling with supernetwork theory to analyze how carobon emissions are transmitted across China's regions and sectors. In this framework, nodes represent regions and sectors via China's economy, and superedges capture the carbon flows between region-sector combinations. This approach departs from traditional flow quantification by uncovering the structural mechanisms and systemic drivers of carbon lock-in across China's regional and sectoral coupled networks. Using this framework, carbon flow networks are analyzed from 2007 to 2017 across 30 regions and 42 economic sectors, identifying key features from three perspectives. Node-level insights identify functionally differentiated actors such as upstream carbon suppliers, downstream consumption hubs, and structural intermediaries, each playing distinct roles in national carbon flows. Superedge-level investigations detect critical region-sector linkages with broad systemic influence or deep structural embeddedness, revealing heterogeneities in decarbonization leverage. Topological structure analysis traces the evolution of carbon-intensive agglomerations, regional clusters, and core-periphery patterns, offering dynamic views of structural carbon lock-in and reconfiguration trends.

The main contributions of this study are as follows. First, we introduce a structurally explicit method to characterize the mechanics of embodied carbon flows at high resolution, enhancing the analytical power of MRIO-based models. Second, we generate actionable insights for network-sensitive carbon governance that target systemic leverage points rather than merely high-emission magnitudes. Third, by integrating spatial, sectoral, and temporal dimensions, we provide a robust analytical foundation for China's differentiated low-carbon transition and clarify the scope of transferability. Although the empirical analysis centers on China, the conclusions are mechanism-level and thus transferable to other large developing economies where extensive interregional trade, heterogeneous energy mixes, and sectoral specialization give rise to similar structures, namely, upstream emitters in resource-rich provinces, downstream sinks in demand-intensive sectors (e.g., construction), and bridge regions connecting inland supply with coastal demand. This transferability is context-dependent; in systems with already low-carbon electricity or limited interregional exchanges, such asymmetries and redundancies may be less pronounced.

2 Methodology

2.1 Carbon flow calculation

Carbon intensity between regions and sectors are calculated based on MRIO tables[27,54], which represents the amount of carbon dioxide emitted per unit of economic output.

$$E_x = CE_x / T_x, \quad x \in \{r, s, (r,s)\} \tag{1}$$

Where E_x represents the carbon intensity, CE_x represents the total carbon emissions, , which is sourced from the CEADs database [55,56], and T_x represents the total output. r denotes region, s sector, and (r,s) a region-sector pair. When an aggregated sector requires subdivision, it assumes that sub-sector emissions scale proportionally with their economic output, ensuring that total emissions are conserved within each region.

The direct carbon flows are then obtained by mapping intensities from the origin to monetary transactions in the MRIO use matrix U.

$$F_{i \to j} = E_i U_{i,j} \tag{2}$$

Where $F_{i \to j}$ represents the direct carbon flows from i to j, i and j can be regions, sectors, or region-sector combinations. This general expression covers the four flow types used in later analysis: region→region, sector→sector, region→sector, and sector→region.

2.2 Carbon flow supernetwork construction

Based on carbon flow calculations, we construct a supernetwork model to capture the multi-layered and heterogeneous interactions of carbon emissions across China's regional–sectoral system. Two intra-layer subnetworks are first established. Using MRIO tables from 2007, 2010, 2012, 2015, and 2017, we quantify carbon emissions across 30 regions and 42 sectors. This enables the construction of a regional subnetwork that reflects spatial carbon flow patterns and a sectoral subnetwork that reveals inter-sectoral emission transfers. Subsequently, two inter-layer subnetworks are developed to characterize cross-dimensional interactions. By computing carbon flows between regions and sectors based on direct emission intensities and monetary transactions, we establish region–sector coupling networks that map how regional/sector activities in one sector/region contribute to carbon flows in another. These inter-layer subnetworks capture the heterogeneous dependencies linking spatial and industrial systems within China’s carbon economy. Four subnetworks form a carbon flow supernetwork that represents horizontal (within-layer) and vertical (cross-layer) connections. This integrated framework enables the identification of structural lock-in patterns that govern the transmission of carbon across China's economy. Table 1 summarizes the mathematical specifications of the three core subnetworks that comprise the supernetwork framework.

Table 1| Subnetwork specifications of the carbon flow supernetwork

	Regional subnetwork	Region-sector subnetworks	Sectoral subnetwork
Node set	$V^{RR}=\{R_1,R_2,...,R_m\}$	$V^{RS}=\{RS_{kl} \mid 1\le k\le m, 1\le l\le n\}$	$V^{SS}=\{S_1,S_2,...,S_n\}$
Edge set	$E^{RR}=\{e_{r_1r_2} \mid 1\le r_1,r_2\le m\}$	$E^{RS}=\{e_{rs} \mid 1\le r\le m, 1\le s\le n\}$	$E^{SS}=\{e_{s_1s_2} \mid 1\le s_1,s_2\le n\}$
Weights	$w_{r_1r_2}^{RR}=F_{r_1,r_2}$	$w_{r_1s_1}^{RS}=F_{r_1,s_1}$, $w_{s_1r_1}^{RS}=F_{s_1,r_1}$	$w_{s_1s_2}^{SS}=F_{s_1,s_2}$

Notes: The regional subnetwork captures interprovincial carbon exchanges, the region–sector subnetworks describe cross-layer couplings between producing regions and consuming sectors, and the sectoral subnetwork represents inter-sectoral carbon flows within the national economy. Weight terms denote embodied carbon flows.

According to supernetwork theory[57-61], a supernetwork can be described as $SN=(V,SE)$, where V represents the node set and SE denotes the superedge set. Accordingly, The carbon flow supernetwork in this study can be expressed as $CFSN=\{V(CF),SE(CF)\}$. Here, $V(CF)$ denotes the node set, consisting of two heterogeneous node types—regions and sectors. $SE(CF)$ represents the superedge set, where each superedge connects nodes from different domains, capturing carbon flows between regions and sectors. In this framework, a superedge corresponds to a carbon flow relationship that links regional and sectoral nodes from heterogeneous networks. Two types of carbon flows are modeled: region-to-sector flows and sector-to-region flows. This design extends conventional MRIO-based networks by embedding bidirectional, cross-layer interactions as structural units of analysis. Since MRIO tables are monetary transaction matrices, the carbon flows inherently embed economic flows together with physical emissions, meaning that the constructed carbon flow supernetwork simultaneously reflects both economic and environmental interactions. Such formulation allows the model to trace the directional movement of carbon between production and consumption nodes, revealing key transmission paths and structural dependencies.

The supernetwork enables the identification of sectoral usage patterns, regional emission responsibilities, and the complex interdependencies across multi-layered economic systems. In total, the carbon flow supernetwork comprises 30×42 region–sector pairs. To manage computational complexity and highlight significant transmission pathways, a magnitude-based pruning technique is employed. This method sparsifies the network by removing low-weight connections while preserving critical carbon flows, thereby improving computational efficiency without compromising structural accuracy [62-64]. Although constructed from static MRIO tables, the multi-year design of the supernetwork allows us to trace observed improvements in production efficiency and structural adjustments across time.

2.3 Carbon flow supernetwork evaluation

To systematically characterize the properties of the carbon flow supernetwork, this study employs a set of network metrics categorized into node-level, superedge-level, and structural-level analyses. Each set of metrics captures different aspects of the carbon flow system, from local connectivity to system-wide structural influence.

Degree measures the number of direct connections of a node, reflecting its role as a source (out-degree) or sink (in-degree) of carbon flows [65].

$$ISD_i = \sum_{i=1} a_{ji} \quad (3)$$

$$OSD_i = \sum_{j=1} a_{ij} \quad (4)$$

Where $A = \{a_{ij}\}$ is the adjacency matrix, $a_{ij} = 1$ or 0.

Betweenness centrality [66] captures the extent to which a node lies on the shortest paths between other nodes, indicating its function as an intermediary.

$$VB_i = \sum_{x \neq i \neq y} g_{xy}^i / ga_{xy} \tag{5}$$

where ga_{xy} represents the total number of shortest paths from node x to y, g_{xy}^i denotes the number of these shortest paths passing the node i.

Eigenvector centrality [67] accounts for both the number and importance of connected neighbors, assigning higher scores to nodes linked to other central nodes.

$$EC_i = \frac{1}{\lambda} \sum_{j=1} a_{ij} \cdot EC_j \tag{6}$$

Where λ is the eigenvalue of the adjacency matrix, which is a constant. EC_j represents the eigenvector centrality of node j which is adjacent to node i.

Superedge connectivity (SUC)[68] quantifies the breadth of influence by measuring how extensively a given superedge (a directed carbon flow from one region-sector pair to another) connects to other parts of the network.

$$SUC_{SE1} = \sum_{SE1(SE1 \neq SE2)}^{sn} \sum_{i=1}^{m \times n} (e_{i,SE1} \times e_{i,SE2}) \tag{7}$$

Where sn is the total number of superedges in the carbon flow supernetwork, and $m \times n$ ($m = 30$, $\mathrm{n} = 42$) is the total number of superedges in the carbon flow supernetwork. $EE = \left(e_{i,SE1}\right)$ is the superedge association matrix of the carbon flow supernetwork, which is described as $EE = \left(e_{i,SE1}\right) = \begin{bmatrix} e_{1,1} & e_{1,2} & \cdots & e_{1,sn} \\ e_{2,1} & e_{2,2} & \cdots & e_{2,sn} \\ \vdots & \vdots & \ddots & \vdots \\ e_{30,1} & e_{30,2} & \cdots & e_{30,sn} \end{bmatrix}$. If node i both belongs to superedges $SE1$ and $SE2$, then $e_{i,SE1} \times e_{i,SE2} = 1$.

Superedge similarity (SUS) [60] evaluates the depth of influence, assessing the degree to which one superedge shares common interaction patterns with others.

$$SUS_{SE1,SE2} = \frac{\sum_{i=1}^{m\times n}(e_{i,SE1} \times e_{i,SE2})}{\sum_{i=1}^{m\times n}(e_{i,SE1} + e_{i,SE2})} \tag{8}$$

$$SUS_{SE1} = \sum_{SE1(SE1\neq SE2)}^{sn} SUS_{SE1,SE2} / sn - 1 \tag{9}$$

Where $SUS_{SE1,SE2}$ denotes the SUS between superedges $SE1$ and $SE2$. SUS_{SE1} denotes the SUS of superedge $SE1$.

The k-core decomposition[69,70] identifies densely connected subgraphs within the carbon flow supernetwork, which represent core regional-sectoral clusters that drive carbon flow aggregation.

$$\forall(d_{n-|H|}) \geq k \tag{10}$$

Where $d_{n-|H|}$ is the degree of node i in the network $N^* = (N-E, E-L)$, k is a constant, $H = \{i \mid SD_i < k\}$, $L = \{(i,j) \mid SD_i, SD_j < k\}$, $SD_i = ISD_i + OSD_i$.

The cycle degree of node i refers to the number of directed cycles passing through it, while the cycle length of a directed cycle is defined as the number of edges in that cycle[71].

$$\alpha(i) = \sum_{s=1}^{c} \alpha^{l_s}(i) \tag{11}$$

$$l(i) = \frac{\sum_{s=1}^{c} l_s(i) \times \alpha^{l_s}(i)}{\alpha(i)} \tag{12}$$

Where $\alpha(i)$ denotes the number of directed circle passing the node i, $\alpha^{l_s}(i)$ is the circle length of node i, whose cyclomatic number is $l_s(i)$, and $l(i)$ is the average circle length.

Network density[72] reflects the degree of connectivity between region–sector nodes by measuring how closely the actual structure approximates a fully connected graph.

$$\rho = sn / v(v-1) \tag{13}$$

2.4 Data sources and consolidation

Time-series MRIO tables are used to calculate carbon flows of the Chinese economy. The MRIO data for the years 2007, 2010, 2012, 2015, and 2017 are obtained from the China Emission Accounts and Datasets (CEADs), as compiled by Zheng et al[36]. The MRIO tables cover 30 administrative regions, including 22 provinces, 4 municipalities, and 4 autonomous regions (Table A.1), and are disaggregated into 42 economic sectors per region (Table A.2). Although CEADs MRIO tables are already standardized to 42 sectors, minor inconsistencies exist in 2017 vintage because of adjustments in industrial codes by the National Bureau of Statistics. To ensure temporal comparability, the 2017 sectors were harmonized to the earlier scheme (Table A.2) by merging the two R&D-related categories and reinstating waste sector through proportional reallocation based on 2015 shares. This choice of MRIO tables for above years is determined by the current availability of China's input-output databases. The most recent official multi-regional input-output data for China is updated only through 2017. Although model-based estimates for subsequent years are available, they lack calibration by authoritative institutions and broad industry consensus. To ensure data quality and the robustness of this study, such estimates are not adopted.

All MRIO tables were converted to 2007 constant prices using province-level GDP deflators obtained from the National Bureau of Statistics. For each province r, the deflation coefficient was defined as $D_{r,t} = GDP_r^{2007} / GDP_r^t$, where GDP_r^t is nominal GDP in year t. Each monetary element of the MRIO matrix was multiplied by $D_{r,t}$ to remove inflationary effects, ensuring comparability of economic flows and emissions across years.

To ensure that the consolidation of multiple MRIO vintages does not bias the network structure, two sensitivity tests were performed. The first test used alternative base-year deflation with 2010 RMB prices, while the second adjusted energy-intensive sector emissions by $\pm 10\%$ to test non-proportional emission allocation. Detailed information are provided in Supplementary Text S1.

3 Results

3.1 Carbon flow patterns between regions and sectors

Figure 1 illustrates the two-way carbon flows between regions and sectors in China from 2007 to 2017, depicting how carbon emissions are transmitted from emitting regions to specific sectors (Figure 1a), and how key sectors contribute to regional carbon inflows (Figure 1b). These visualizations highlight regional and sectoral asymmetries of China’s carbon economy and the changing dominance of emission-intensive flows across time. Figure 1a shows that carbon flows are primarily sourced from coal-abundant northern regions, especially Hebei (HE), Shanxi (SX), and Inner Mongolia (NM), toward high-emission sectors such as nonmetal (S13), metal (S14), and electricity (S25). These regions act as upstream suppliers within the national production network, a role shaped by their resource endowments and industrial specializations. In other words, these upstream roles are closely related to the regions’ abundant coal reserves and their policy-driven positions as national energy bases, which are indirectly captured in the MRIO structures. Accordingly, the identified “lock-in” should be understood as a structural dependence shaped by resource-policy contexts, rather than as a denial of potential transition opportunities. The persistence of upstream emitter provinces such as Inner Mongolia and Shanxi also raises issues of carbon equity, as these regions disproportionately bear the burden of carbon-intensive production that serves national demand. From 2007 to 2015, the largest carbon flow was from Hebei to S14, rising from 9.24% to 10.98% of total regional emissions, highlighting Hebei’s strong industrial base and high emission intensity. By 2017, however, the largest flow shifted to Inner Mongolia to S25, suggesting a structural transition linked to increasing energy production capacity and investment in that region. Shanxi to S25 remained the third-largest flow throughout the period; although absolute emissions declined from 26.35 Mt CO_2 (2012) to 23.67 Mt CO_2 (2017), its share of total outflows increased from 8.03% to 8.88%, due to the broader national decline in regional-to-sector carbon transfers post-2012. This result, on the one hand, highlights how structural decline in national emissions can amplify the proportional contribution of key regional emitters. On the other hand, regional prominence in carbon networks is not solely dependent on emission volume, but also on broader systemic changes in interregional trade and energy demand. Additional shifts include the decline of Shanxi to S14, which peaked at 9.63 Mt CO_2 in 2007 and dropped continuously after 2010, and the resurgence of Liaoning (LN) to S25, which decreased from 6.32 Mt CO_2 in 2007 to 2.99 Mt in 2012, but rose again after 2015 by 4.15 Mt CO_2, reflecting localized sectoral reactivation.

Figure 1b illustrates how carbon-intensive sectors redistribute emissions toward regions via interregional trade, capturing consumption-driven carbon demand. S25 remained the dominant exporter of carbon flows throughout the decade, particularly toward coastal economic regions. Between 2010 and 2015, S25 to Shandong (SD) was the largest carbon flow, peaking at 37.55 Mt CO_2 in 2010 due to strong industrial demand. By 2017, however, the flow had significantly decreased, and Jiangsu (JS) surpassed Shandong as the top importer, reflecting the shifting geography of energy-driven emissions toward economically dynamic eastern regions. S14 ranked second in carbon exports. Hebei led as the primary recipient in 2007 and 2012, with an annual growth rate of 16.63%, but was later overtaken by Jiangsu, whose import growth from S14 accelerated to 25.81% per year from 2010 onward, suggesting an intensifying concentration of heavy industrial activity in the eastern coastal belt. S13 consistently ranked third. Its exports to Shandong led in 2007 (5.12 Mt CO_2), dropped sharply in 2010 (2.15 Mt), rebounded thereafter, but were overtaken by Guangdong (GD) in 2017, reflecting evolving construction and infrastructure demand patterns. Persistent spatial decouplings between carbon emissions and final consumption are traced from these patterns. Northern interior regions like Shanxi, Inner Mongolia, and Hebei, accounted for 34.81% of total regional outflows, acting as primary carbon suppliers due to their dependence on energy and heavy industries. In contrast, eastern coastal regions such as Jiangsu, Guangdong, and Shandong, functioned as carbon importers, driven by high demand for electricity, processed materials, and construction inputs. Notably, just five regions received nearly 64% of carbon outflows from S25, highlighting their centrality in downstream consumption and redistribution. This spatial asymmetry between production and consumption underscores the urgency of rethinking carbon responsibility frameworks.

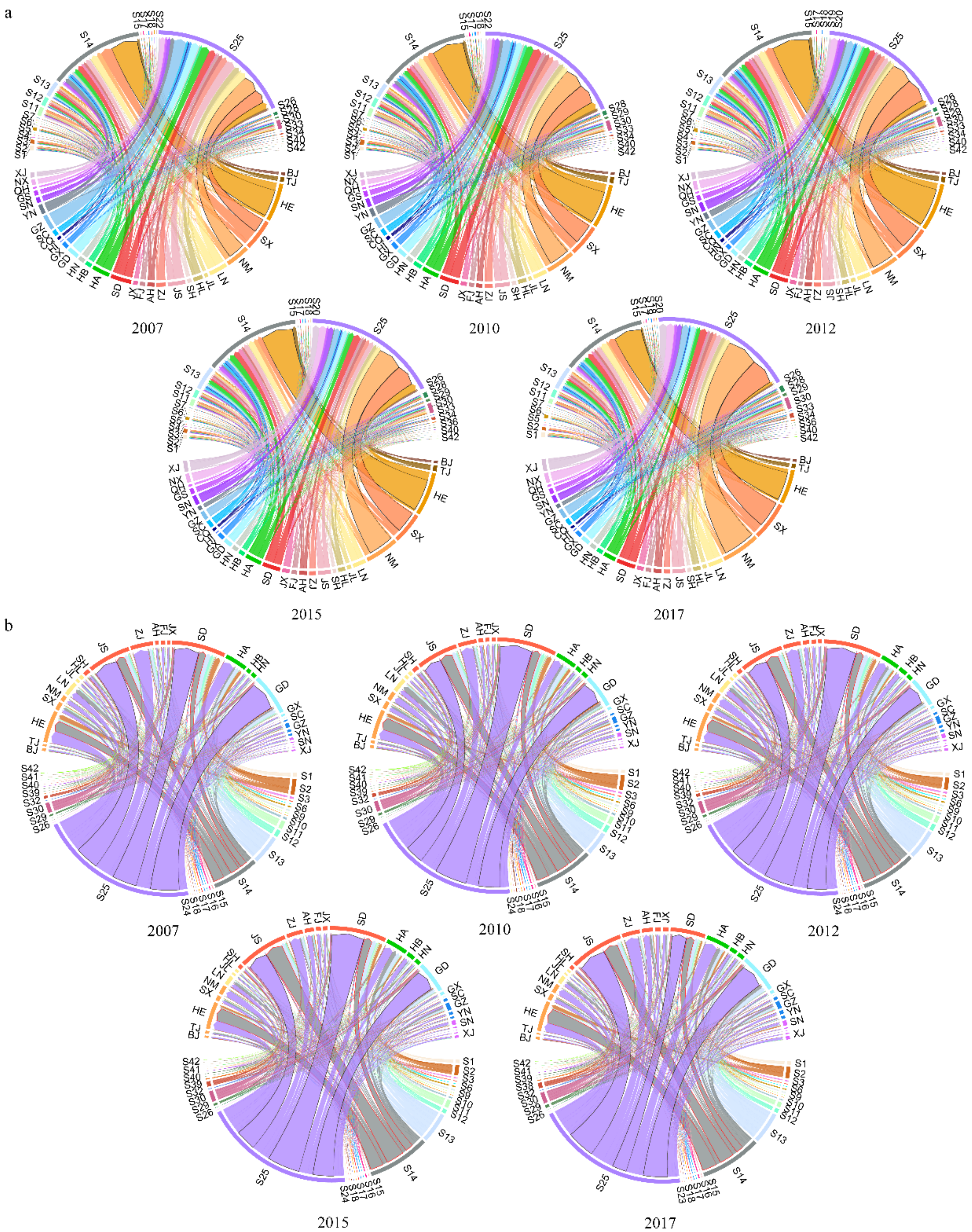

Figure 1| Carbon flows between regions and sectors in China from 2007 to 2017.

Notes: Regions and sectors are detailed in Table A.1 and Table A.2. The width of each chord represents the magnitude of embodied carbon flows (Mt CO_2) between region-sector pairs.

3.2 Node characteristics and regional-sectoral functional roles

Figure 2 presents the top ten regions and sectors across node-level metrics including in- and out-degrees, betweenness and eigenvector centralities from 2007 to 2017, which offers insights into the hierarchical positioning and functional roles of different nodes in carbon flow via China’s economy. At the regional level (Figure 2a), southeast coastal regions such as Shandong (SD), Jiangsu (JS), Zhejiang (ZJ), and Guangdong (GD) account for approximately 50% of Top 10 nodes across most metrics and years, indicating their stable roles as major hubs for carbon inflow and redistribution. This pattern reflects the long-standing economic leadership of coastal regions, where industrial clusters, advanced infrastructure, and international trade have created strong pull effects for embodied carbon flows. These regions serve as terminal nodes for carbon-intensive products, suggesting strong embeddedness within the national carbon flow system. Central regions like Henan (HN) and Hubei (HB) contribute roughly 30% of Top 10 appearances, and show a gradual strengthening of network positions over time. This shift can be attributed to national policies promoting the development of central regions (e.g., the Rise of Central China Plan), coupled with industrial relocation from coastal areas, leading to greater integration of central provinces into national production and trade networks. Northeast regions, represented by Liaoning (LN), appear prominently in out-degree metrics but are largely absent from in-degree and centrality-based rankings. This indicates a structurally defined role as upstream carbon exporters, rooted in the region’s concentration of heavy industries, resource extraction, and basic material processing. The absence of centrality metrics suggests limited integration into broader redistribution networks, reinforcing Northeast China’s profile as a specialized supplier rather than an intermediary hub. Other regions, including Hebei (HE) and Sichuan (SC) are observed in Top 10 rankings across all metrics and years. These two regions exemplify how strategically located inland regions contribute to the national carbon network, both as production bases and as critical connectors bridging eastern and western flows. The regional rankings exhibit high temporal stability over 2007–2017, as evidenced by the persistent dominance of key coastal regions across multiple metrics. This implies persistent spatial carbon lock-ins despite broader economic transitions and policy-driven efforts toward structural transformation, highlighting the entrenched nature of carbon-intensive pathways at the regional level. This temporal persistence of dominant regions indicates not only static stability but also a dynamic lock-in process, whereby historical industrial configurations and policy incentives reinforce the continuity of carbon-intensive pathways over time.

At the sectoral level (Figure 2b), heavy industries and production services dominate China's carbon flow supernetwork, accounting for approximately 70% of Top 10 nodes. Heavy industries such as chemistry (S12), nonmetal (S13), and metal (S14) supply essential materials for downstream construction, manufacturing, and infrastructure. Their sustained dominance reflects the persistent reliance of China's economy on carbon-intensive material production, a key challenge for national decarbonization efforts. Production service sectors, including wholesale and retail (S29), transport and logistics (S30), and information and technology (S32), play increasingly central roles, particularly in recent years. This reflects the ongoing transition toward a more interconnected, service-driven industrial structure, where logistics, digital infrastructure, and market systems increasingly mediate embodied carbon dynamics. Energy industry, especially electricity (S25), is highly prominent in out-degree metrics across all years, contributing about 30% of Top 10 rankings in this dimension. As the primary carrier of energy in modern production and consumption, the electricity sector naturally drives extensive embodied carbon outflows across the entire economy, particularly given China's coal-based energy mix over this period. Agriculture (S1) consistently appears in Top 10 rankings across multiple metrics and years. While not a dominant hub in the carbon network, agriculture contributes significant baseline carbon flows through primary production and food supply chains, highlighting the importance of integrating land-based sectors into comprehensive mitigation strategies. Construction (S28) shows high in-degree and eigenvector centrality, reflecting its dependence on upstream inputs and its centrality within the national carbon flow supernetwork as a major end-use sector. However, its low betweenness centrality reflects its role as a terminal demand sector, primarily absorbing carbon flows rather than mediating interregional exchanges. The stability of top sectors over the decade, particularly infrastructure-heavy sectors, indicates low degrees of sectoral decarbonization. This highlights difficulties of shifting away from structurally embedded high-carbon activities, as these sectors remain central to economic functionality and carbon network dynamics. The rising prominence of production services, alongside the sustained dominance of heavy industries, reflects not only static structural reliance but also the dynamic process of industrial upgrading and demand transformation, which gradually reconfigures the carbon flow system. Their persistence underscores the need for targeted, sector-specific interventions to achieve meaningful decarbonization within the embodied carbon system.

While the node analysis isolates regional and sectoral roles, it cannot reveal their integrated positions. By linking the regional and sectoral attributes, we identify that Inner Mongolia-electricity (S25) exemplifies a resource-dependent upstream anchor. Although Inner Mongolia does not rank among the top network hubs (Figure 2), it remains one of the largest carbon emitters nationwide and a dominant supplier of coal-based electricity. In 2017, this combination accounted for approximately 10% of total region-to-sector carbon flows, underscoring its pivotal role as a structural emission source rather than a network intermediary. Its lock-in mechanism is resource-driven: abundant coal endowments, long-term energy-base policies, and sunk investments in power infrastructure jointly sustain a carbon-intensive production regime. Such peripheral lock-in reveals that even non-central nodes can exert systemic influence by anchoring the carbon supply side of the network. By contrast, Jiangsu-Metal (S14) represents a demand-driven downstream hub. It contributes about 8 % of total sector-to-region carbon inflows, reflecting Jiangsu's industrial demand for metal materials in manufacturing and construction. Its lock-in is consumption-driven: agglomerated heavy-industry demand, supply-chain integration, and material-intensive urbanization reinforce embodied-carbon inflows from upstream provinces. This combination shows high in-degree and eigenvector centrality but limited out-degree, identifying Jiangsu as a terminal consumer node consolidating emissions rather than mediating them. These cases reveal two complementary mechanisms of regional-sectoral carbon lock-in: resource-based inertia in inland, energy-rich provinces that sustain upstream emissions through infrastructural and policy entrenchment, and demand-aggregation inertia in coastal manufacturing hubs that perpetuate downstream carbon inflows. Recognizing these differentiated pathways can clarify how source- and sink-side structures jointly reproduce China's high-carbon development trajectory.

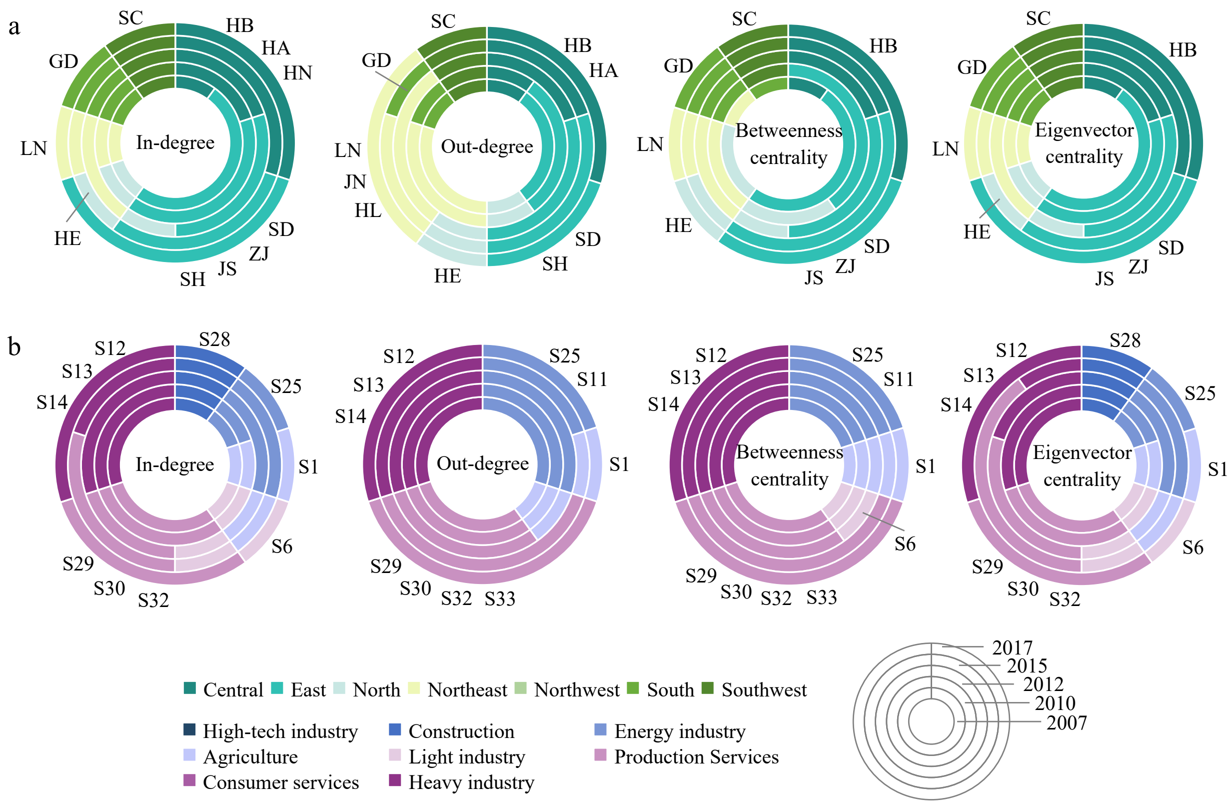

Figure 2| Top 10 regions (a) and sectors (b) in node-level metrics during 2007-2017

Note: Each ring represents a year (2007-2017), moving outward chronologically.

3.3 Superedge influence and heterogeneous carbon flow interactions

To assess how specific regional-sectoral connections (superedges) shape the structure and stability of China's carbon flow system, we evaluate two critical superedge-level metrics of superedge connectivity (SUC) and superedge similarity (SUS). SUC reflects the breadth of a superedge's systemic influence, i.e., the extent to which a region-sector connection radiates across the network. In contrast, SUS captures the depth of its interactions, indicating how strongly a superedge aligns with the behavioral patterns of others. Figure 3 presents the top 25 superedges ranked by SUC and SUS from 2007 to 2017.

The highest SUC-ranked superedges are predominantly composed of connections between coastal economic centers and high-technology or consumer service industries (Figure 3a). For example, superedges such as GD-S27 (Guangdong-water), JS-S23 (Jiangsu-waste recycling), and ZJ-S21 (Zhejiang-instrumentation) dominate the top SUC rankings. These superedges represent critical pathways through which carbon flows are orchestrated across multiple regional and industrial domains. The dominance of these superedges reflects scale effects in coastal hubs, where provinces such as Guangdong, Jiangsu, and Zhejiang concentrate industrial agglomeration and diversified demand, anchoring large embodied flows that link upstream energy- and material-intensive sectors with downstream technology and services. Their high connectivity reveals their systemic importance in stabilizing carbon transmission under policy interventions, such as efficiency upgrades and low-carbon transitions, and highlights their potential as leverage points for large-scale carbon reduction efforts. Over time, a distinct evolution is observed in the composition of top-ranking SUC superedges. In the early years (2007–2010), superedges dominated by consumer services and traditional production industries were more prominent. However, by 2012 and beyond, there is a clear transition towards high-technology industries and advanced service sectors, paralleling China's broader economic shift towards services and innovation-driven development. Spatially, the leadership of SUC superedges also becomes increasingly concentrated within eastern coastal regions, reflecting their growing dominance in coordinating nationwide carbon flows. High-SUC superedges serve as broad leverage points: cutting coastal demand intensity, raising efficiency, and expanding low-carbon services can diffuse mitigation benefits across the supernetwork without intervening in every peripheral link.

In contrast, the highest SUS-ranked superedges exhibit greater temporal stability and are largely concentrated in heavy industries and production services within southeastern coastal regions (Figure 3b). Superedges such as SD-S13 (Shandong–nonmetal) and SD-S25 (Shandong–electricity) consistently top SUS rankings, indicating deeply embedded, structurally aligned carbon exchanges rooted in Shandong's industrial complex. Other high-SUS superedges like SD-S28 (construction), SD-S30 (transport and logistics), and SD-S32 (information and technology) further illustrate Shandong's multi-sectoral entrenchment within the carbon flow supernetwork, highlighting its centrality in both material production and service intermediation. This persistence reflects the convergence of several forces: industrial agglomeration in heavy-industry and producer-service complexes, supply-chain complementarity between upstream energy/material inputs and downstream construction/services, and policy-driven roles of coastal provinces as national hubs. Together, these mechanisms reinforce overlapping carbon exchanges, which SUS detects as structurally aligned and persistent couplings. Temporal analysis shows that while the sectoral structure of high-SUS superedges remains stable, spatial diffusion becomes more evident in later years, with central and southwestern provinces such as Henan (HA) and Sichuan (SC) increasingly entering the SUS top ranks. This suggests a slow but steady embedding of inland industrial centers into national carbon flow patterns, mirroring broader trends of industrial relocation and inland development policies. High-SUS superedges linking inland energy bases to coastal demand centers further reflect equity concerns, where production-side provinces incur concentrated emissions while consumption-side provinces externalize their embodied carbon. From a governance perspective, such high-SUS couplings imply both risks and opportunities: they magnify policy transmission if interventions target key flows, but also raise lock-in risks if left carbon intensive. Addressing these superedges therefore requires upstream decarbonization, demand-side standards in construction, and selective re-routing of critical couplings, while monitoring inland diffusion to avoid reproducing coastal lock-in patterns.

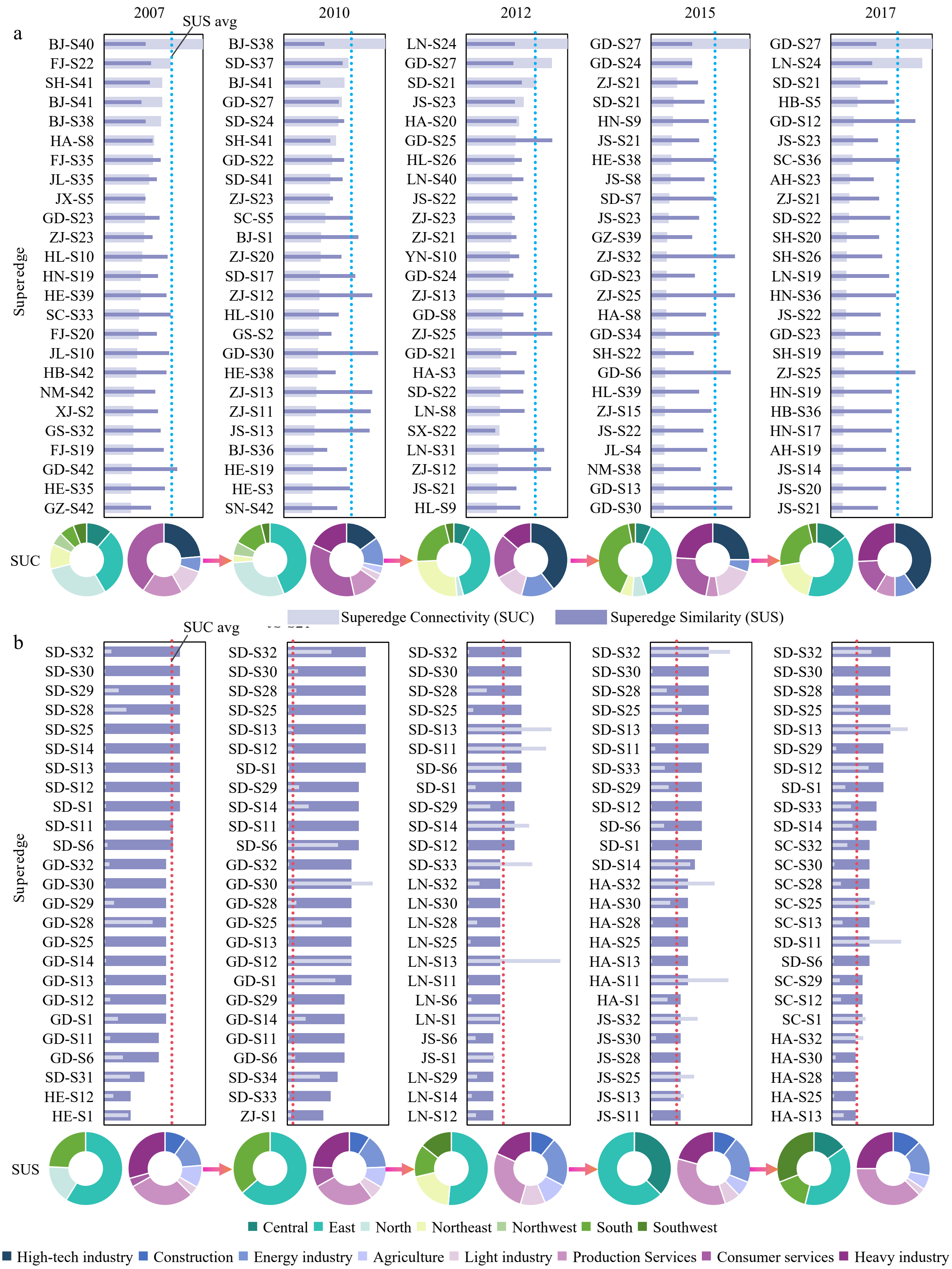

Figure 3| Top 25 superedges and corresponding regional and sectoral categories ranked by superedge connectivity (SUC) (a) and superedge similarity (SUS) (b) during 2007-2017

Note: Circular diagrams summarize the compositional evolution of superedges across seven regions (left) and eight sectoral categories (right).

Further examination reveals substantial functional heterogeneity between SUC and SUS superedges. Approximately 87% of superedges display an inverse relationship between SUC and SUS values. Superedges like SD-S28, ZJ-S30, and HE-S12 feature high SUS but relatively low SUC, reflecting deep but localized influence, often tied to strong industrial agglomeration and concentrated demand within specific regions. In contrast, superedges such as ZJ-S21, SH-S20, and BJ-S31 exhibit high SUC but lower SUS, indicating broad yet shallow carbon interactions associated with standardized services and technology-driven sectors. These insights emphasize two strategic paths for optimizing carbon flows within heterogeneous networks. Enhancing technological upgrading and carbon efficiency in deeply embedded, high-SUS superedges to maximize decarbonization leverage within regional cores, and promoting structural transitions toward high-value, low-carbon service and technology sectors in high-SUC but low-SUS superedges to expand the breadth of carbon reductions across the system. Such differentiated strategies, informed by superedge roles, are critical for overcoming carbon lock-in challenges and achieving national carbon neutrality objectives.

3.4 Structural agglomeration and core regional-sectoral clusters

To examine the structural agglomeration and identify core nodes within China's carbon economy, we apply k-core decomposition to reveal cohesive substructures that form the backbone of interregional carbon flows. As shown in Figure 4, the k-core subgraphs from 2007 to 2017 remain largely stable, despite slight annual variation in the maximum k-values (ranging from 28 to 30), indicating a robust structural hierarchy. We found two distinct regional groupings embedded in high-order cores. First, economically advanced regions, including Tianjin (TJ), Hebei (HE), Shanghai (SH), Jiangsu (JS), Zhejiang (ZJ), Anhui (AH), and Guangdong (GD), persistently remain in the innermost cores across all years. These regions constitute the economic centers of China's dominant urban clusters: Jing-Jin-Ji and the Yangtze River Delta. Their centrality in the k-core reflects high industrial density, strong cross-regional trade integration, and embedded infrastructure demand, positioning them as structural stabilizers in the carbon flow network. Strategically enhancing integration and decarbonization within these hubs may yield broad system-level efficiency gains and emission reduction spillovers. Second, a group of resource-dependent yet economically less-developed regions, notably Inner Mongolia (NM), Liaoning (LN), Jilin (JN), Heilongjiang (HL), and Henan (HA), also maintain stable inclusion in the k-core. Despite lower degrees of economic agglomeration, their roles as upstream suppliers of energy and heavy industrial inputs ensure their structural significance. These regions exhibit persistent high carbon emissions due to reliance on coal-intensive sectors and limited diversification. Their inclusion in the core highlights the challenge of economic-environmental decoupling, where emission growth outpaces productivity gains. Addressing this imbalance requires local policy shifts and coordinated governance efforts to support structural transformation and green capacity building in these high-emission hinterlands.

The sectoral composition of stable k-cores consists of a combination of high-carbon, foundational industries, including agriculture (S1), energy industries (coal mining (S2), petroleum and nuclear fuel processing (S11), electricity (S25)), heavy industries (chemistry (S12), nonmetal (S13), metal (S14)), construction (S28), and production services (wholesale and retail (S29), transport and logistics (S30), information and technology (S32), Finance (S33)). The persistence of these sectors in the k-core over a decade highlights a structural path dependency on resource- and emission-intensive activities. While these sectors underpin economic output and supply chain continuity, their centrality also signals vulnerability to carbon lock-in. Transitioning toward sustainable growth thus requires not only end-of-pipe mitigation, but systemic restructuring, such as industrial upgrading, energy substitution, and cross-regional green technology diffusion, to break structural inertia.

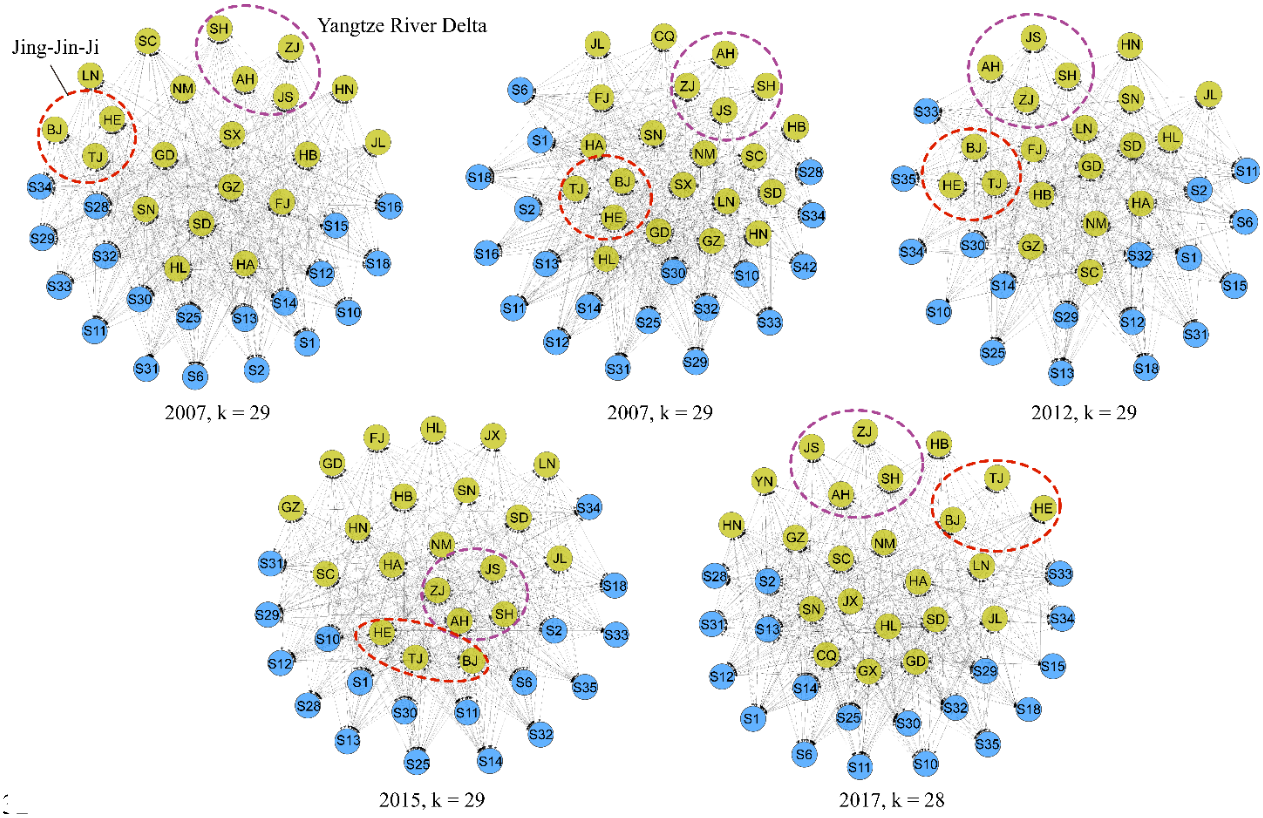

Figure 4| k-core structures of China's carbon flow supernetwork

Notes: Yellow nodes represent regions and blue nodes represent sectors. Red and purple dashed circles highlight two persistent core clusters: the Jing-Jin-Ji (Beijing-Tianjin-Hebei) and Yangtze River Delta (Shanghai-Jiangsu-Zhejiang-Anhui).

3.5 System stability and internal carbon cycling

Figure 5 illustrates the temporal evolution of network density, capturing changes in the overall interconnectivity of regions and sectors. The network density increased from 0.200 in 2007 to a peak of 0.231 in 2015, indicating enhanced interconnectivity among regions and sectors. This growth reflects more intensive carbon exchange and stronger economic linkages, suggesting a more integrated and efficient carbon flow system during this period. The rise in density also corresponds with the emergence of more connected subgraphs, pointing to improved systemic cohesion within the network, likely driven by accelerated industrialization and infrastructure expansion. However, by 2017, network density declined to 0.218, marking a structural turning point. This reduction aligns with China's strategic pivot from high-speed growth toward green transformation. As low-carbon policies began constraining high-emission sectors, interregional carbon transfers became less diffuse, reducing the breadth of certain carbon linkages. The evolution of network density thus reflects a trade-off between economic integration and climate-oriented restructuring, where structural decarbonization reshapes the topology of carbon connectivity.

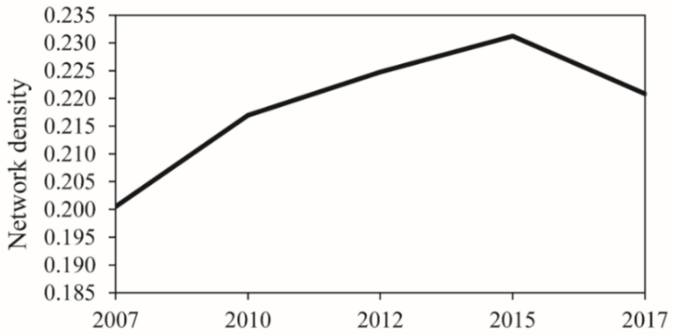

Figure 5| The network density of China's carbon flow supernetwork

Complementing the density trend, Table 2 presents annual node-level cycle participation to reveal the capability to sustain and facilitate the internal circulation of carbon emissions within economic agglomerations. Regionally, most regions maintained high levels of cycle involvement (exceeding 35,000 cycles annually), highlighting their foundational role in sustaining local carbon flow feedback loops. Shandong dominated in cycle frequency from 2007 to 2015, underscoring its centrality in production and redistribution activities. However, by 2017, its ranking dropped to sixth, suggesting a potential shift in regional carbon exchange dynamics. In contrast, Zhejiang and Guangdong consistently ranked among the top regions, reflecting their enduring integration within coastal agglomerations. Henan saw a marked rise in cycle participation in 2015 and 2017, indicating strengthened interregional linkages and an increasingly supportive role in the national carbon system. These regional shifts point to growing structural differentiation and adaptive capacity within the RSCFN. Sectoral node analysis similarly indicates robust cycle participation (over 30,000 cycles annually), reflecting strong sectoral interconnections across regions. From 2007 to 2017, the information technology services (S32) exhibited the most notable increase in cycle involvement, highlighting its rising influence in facilitating technological diffusion, service-driven linkages, and industrial upgrading. Conversely, traditional heavy industries such as chemistry (S12) experienced a steady decline in cyclicity, signaling a reduced ability to support interregional carbon recirculation. This pattern aligns with China's broader structural transition—from carbon-intensive manufacturing to innovation- and knowledge-driven sectors—as a foundation for future sustainable growth. The dual trends of evolving connectivity and shifting cycle participation reveal a carbon flow system undergoing strategic transformation. While structural cohesion initially intensified with economic growth, recent signals suggest a reorientation toward a more selective, low-carbon network architecture. This transition reflects both the pressures and opportunities of systemic decarbonization, where improving internal cycling efficiency and optimizing node connectivity are essential for long-term resilience.

Table 2| Top 5 regional and sectoral nodes in cycle degree

	Cycle degree of regions					Cycle degree of sectors				
Year	2007	2010	2012	2015	2017	2007	2010	2012	2015	2017
Average	39985	40383	39869	40056	35276	32747	33142	33618	32882	30736
Top 5	SD	SD	SD	SD	ZJ	S12	S12	S11	S25	S32
	GD	GD	ZJ	ZJ	SC	S30	S13	S1	S32	S25
	ZJ	ZJ	LN	HA	HA	S13	S25	S25	S11	S13
	SH	SH	HE	GD	HN	S1	S1	S32	S13	S30
	JS	JS	HB	HN	GD	S14	S30	S30	S30	S29

Note: Cycle degree measures the number of closed carbon flow loops in which a node (region or sector) participates, indicating its contribution to feedback structures within the supernetwork. Higher values represent stronger involvement in carbon circulation rather than one-way transmission.

4 Discussion

This study constructs the carbon flow supernetwork to analyze how carbon emissions are spatially and sectorally redistributed across China. The network-based perspective reveals that carbon flow is not uniformly distributed but instead reflects deep structural heterogeneity shaped by regional resource endowments, industrial specialization, and economic agglomeration. Recognizing these structural differences is essential for designing differentiated and targeted carbon reduction strategies that align with the carbon peaking and neutrality goals.

Network metrics underscore that carbon governance must differentiate between embedded hubs and peripheral suppliers. Provinces with central positions sustain demand-driven linkages, while resource-based regions remain upstream providers; effective strategies should therefore go beyond emission volumes and address the structural embeddedness of each node. Superedge metrics reveal complementary pathways for intervention. High connectivity (SUC) identifies links with broad diffusion potential, while high similarity (SUS) signals entrenched dependencies; together they show where to prioritize efficiency standards, fuel switching, and re-sourcing. Hybrid cases are especially instructive: deep but localized superedges require cross-regional cooperation and finance to scale their impact, while broad but shallow ones can steer consumption and innovation toward low-carbon trajectories. The structural backbone of China's carbon economy lies in persistent regional cores that act simultaneously as growth engines and carbon anchors. These clusters demand integrated policies that link technological leadership in core cities with upstream decarbonization and sectoral upgrading across surrounding regions, ensuring coordinated rather than piecemeal transitions. From a carbon equity perspective, the supernetwork analysis also reveals imbalances: upstream provinces disproportionately bear emission burdens while downstream absorbers benefit from embodied inflows. This pattern is consistent with MRIO-based evidence on embodied transfers in China [56,73]. To substantiate this pattern, we quantified interprovincial carbon transfers. Upstream energy- and resource-intensive provinces such as Shanxi, Inner Mongolia, and Ningxia remain consistent carbon exporters, whereas economically advanced coastal provinces such as Beijing, Shanghai, and Guangdong exhibit persistent carbon import dependence (Figure S1; Table S8). In parallel, a carbon equity evaluation matrix (Figure S2) was constructed by combining per-capita GDP and production-based carbon intensity (t CO_2 per 10^4 CNY), using China's annual mean as reference. The matrix identifies four regional archetypes: green leaders (high income, low intensity), transition-intensive (high income, high intensity), inclusive growth (low income, low intensity), and support priority (low income, high intensity). Coastal and metropolitan economies (e.g., Beijing, Shanghai, Jiangsu, Zhejiang) fall in the green leader quadrant, while upstream energy bases (e.g., Shanxi, Inner Mongolia, Ningxia, Guizhou) occupy the support priority quadrant. The convergence of carbon transfers and equity-matrix results reveal persistent structural inequities between economic benefits and emission responsibilities, echoing findings in the broader literature on interregional carbon inequality [74]. Addressing these inequities requires differentiated policy tools—such as transfer payments, green investment incentives, and region-specific transition pathways—that balance responsibilities and capacities across provinces.

The dynamic evolution of China’s carbon system underscores the persistence of path-dependent mechanisms alongside gradual reconfiguration. Changes in network density and cycle participation reflect the evolving cohesion of the carbon system: rising participation of inland provinces and emerging service sectors indicates that new actors are becoming embedded in systemic loops, while traditional heavy industries gradually lose circulation roles. Multi-period analysis (2007-2017) shows enduring coastal hubs, the growing importance of services, and the diffusion of high-SUS superedges from coastal to inland provinces. These dynamics are explained by industrial agglomeration, supply-chain complementarity, and policy-driven specialization, which not only sustain existing lock-ins but also provide leverage points for intervention. High-SUS superedges, such as Shandong’s multi-sector couplings in electricity, construction, and logistics, are rooted in these complementarities and policy-driven specialization, and their diffusion into provinces like Henan and Sichuan demonstrates that lock-in motifs can spread geographically. The shifting roles of inland provinces and emerging services suggest a window of opportunity to steer transition from quantity-driven growth toward innovation-led green development, consistent with lock-in theory that stresses reinforcing mechanisms behind carbon-intensive structures [10,75].

The supernetwork evaluation therefore reframes carbon governance as a structural intervention problem, identifies three categories of actors whose interactions sustain China’s carbon lock-in, and provides a systematic roadmap for breaking carbon lock-in. (1) Upstream supply anchors such as Inner Mongolia-Electricity and Shanxi-Coal, possess high out-degree centrality, exporting over 70% of embodied carbon flows. Structural leverage lies in reducing the emission factor per unit output and weakening the centrality of carbon-intensive superedges. Key measures include tightening efficiency standards for coal- and gas-fired power to $\leq$ 300 gCO_2/kWh by 2030 (−15% from 2020 baseline), and expanding renewable integration in regional grids to $\geqslant$45% electricity share by 2035. These measures directly reduce outflow intensity and shift centrality from energy to cleaner generation nodes, thus dismantling resource-based inertia. (2) Intermediary processors such as Henan-Chemical and Shandong-Transport, balance inflows and outflows (~1.0 ratio) and mediate 30 – 40% of total national carbon transmission. Structural mitigation should focus on clean-process transitions and green supply-chain procurement, mandate low-carbon materials procurement in construction and manufacturing with a minimum 50% clean procurement share by 2030, and promote industrial symbiosis in chemical and transport sectors to reuse by-products and recover waste heat. These actions lower the SUS between energy- and material-intensive sectors by 8-12%, reducing redundant carbon linkages and improving network efficiency. (3) Downstream demand hubs such as Jiangsu-Metal and Guangdong-Machinery, show high in-degree centrality (>0.65) as carbon sinks through final demand. Their leverage stems from demand substitution and electrification of logistics, implement green procurement standards for public and corporate consumers (⩾30% low-carbon products by 2030), and accelerate logistics electrification to achieve 60% zero-emission freight vehicles by 2035. These strategies weaken the inflow dominance of heavy industrial sectors and gradually shift demand toward service-based and renewable-intensive nodes, mitigating demand-driven lock-in (see Table S9 for a summary of structural categories and corresponding interventions). Integrating the network metrics and carbon-flow magnitudes, a leverage-based sequencing can be proposed. Phase I (2025-2030): Upstream mitigation first to decarbonize electricity and metallurgy supply nodes that account for ~40% of total embodied outflows. Phase II (2030-2040): Midstream optimization to strengthen circular manufacturing and green procurement to reconfigure conversion pathways, reducing SUS overlap density by 10%. Phase III (2040-2050): Downstream transformation to reshape consumption and logistics demand, lowering final embodied inflows by 20-25%. This sequenced strategy corresponds to progressive centrality rebalancing. Phase I reduces out-degree dominance of energy sectors, Phase II lowers superedge overlap across heavy industries, and Phase III decreases in-degree aggregation in coastal demand hubs. These shifts produce a systemic contraction of carbon interdependencies, transforming the national economy from a lock-in-prone to a resilient low-carbon configuration (for policy-relevant evidence on interregional reconfiguration, see Wang, et al. [76]).

Besides empirical findings, the study also contributes methodologically. By integrating MRIO with supernetwork analysis, we advance from simply mapping how much carbon flows where to revealing how cross-layer structures sustain flows and where to intervene. Superedges expose bidirectional region-sector dependencies and reveal integrated upstream-downstream roles that are invisible when regions and sectors are analyzed separately. Connectivity and similarity metrics diagnose whether carbon pathways are redundant and concentrated—signatures of structural lock-in—or diversified, which cannot be inferred from MRIO magnitudes or single-layer degrees. Recurrent cross-layer cycles and motifs explain why high-carbon structures persist across years even when technical coefficients improve. These observed lock-in and reconfiguration patterns should be interpreted as topological manifestations of systemic dependence, not as direct policy-induced outcomes. To partially validate the inferred mechanisms, a pre- and post-policy contrast was implemented around the 12th Five-Year Plan (2011-2015), which marked China's first nationwide carbon-intensity control and energy-efficiency campaign. Between 2007-2010 and 2015-2017, network density decreased from 0.214 to 0.193 (−9.8%), while core–periphery disparity reduced by 6.3%, suggesting that structural coupling between upstream energy and downstream manufacturing nodes weakened modestly during the policy period. These changes are consistent with, though not exclusively caused by, policy-driven decarbonization and industrial upgrading. The findings also contribute to theoretical dialogue by distinguishing carbon lock-in from carbon dependency [10,75]. Dependency emphasizes reliance on carbon-intensive resources, whereas lock-in highlights the reinforcing mechanisms that perpetuate such reliance even when alternatives exist. Recognizing both is essential for designing policies that target not only resource reliance but also structural inertia.

Critical region-sector couplings reflect technological heterogeneity within sectors. For example, Inner Mongolia's electricity mix is dominated by coal, whereas Sichuan's relies primarily on hydropower. These fundamental differences in resource endowments and technology mixes shape the carbon intensity of otherwise identical sectors and explain why some region-sector pairs consistently rank as critical superedges. Recognizing such heterogeneity sharpens the interpretation of lock-in: similarities captured by SUS represent not only structural demand-supply couplings but also entrenched technology portfolios. Addressing them requires differentiated measures—fuel switching and efficiency retrofits in fossil-based provinces versus demand substitution and grid integration in renewable-rich provinces. This aligns with updated carbon-lock-in perspectives that integrate technological and institutional dimensions [77].

Despite its contributions, this study is subject to limitations common to MRIO-based analyses. The framework assumes fixed technical coefficients within each year, so although multi-year data reflect observed changes in efficiency and structure, they do so only in a stepwise manner, and the comparative design across discrete time points does not fully capture continuous dynamics of technological change, substitution, or policy feedbacks. External drivers such as energy prices, environmental regulations, and international trade are only implicitly embedded in MRIO data, and while import-export accounts partly reflect international exchanges, our framework does not explicitly model global linkages. Sectoral aggregation may mask important technological heterogeneity, as illustrated by differences between coal-based electricity and hydropower-dominated electricity. Future research could therefore incorporate dynamic MRIO variants or hybrid MRIO-CGE approaches, link the supernetwork framework with explicit policy and trade layers, couple domestic networks with global MRIO databases, and incorporate sub-sectoral and technology-specific data into a region-sector-technology tri-layer design, thereby yielding a more comprehensive picture of carbon lock-in and transition pathways. In addition, extensive uncertainty, sensitivity, and robustness analyses (Supplementary Text, Sections S1-S3) confirm that the network rankings, superedge metrics, and policy-relevant findings remain stable under alternative assumptions, parameter settings, and aggregation levels, supporting the reliability of the findings.

5 Conclusion

This study develops a supernetwork framework to systematically uncover the structural logic and dynamic evolution of carbon flows across China's economy. By integrating MRIO data with network science, we shift from conventional emission accounting to reveal how carbon is embedded, circulated, and locked in through regional-sectotal interdependencies. Our analysis indicates that China's carbon emissions are governed not only by high-emitting regions or sectors but more profoundly by structurally embedded nodes and linkages. We identify three key mechanisms underpinning carbon lock-in. First, upstream emission is concentrated in coal-rich regions that continue to supply carbon-intensive outputs through power and heavy manufacturing. Second, downstream demand is consolidated in industrialized coastal regions, which are carbon consumers and redistribution centers. Third and most critically, a small group of intermediary regions and sectors, including Shandong, Henan, logistics, construction, and information services, exhibit high structural centrality and effectively mediate carbon transfers throughout the national economy. These actors constitute functional bottlenecks and strategic leverage points within the carbon system.

Moreover, structural features such as persistent high-order k-cores in the Jing-Jin-Ji and Yangtze River Delta agglomerations serve as spatial anchors of carbon path dependence, while post-2015 shifts in network density and carbon cycle participation suggest the early emergence of low-carbon transformation pathways centered on service and innovation sectors. These findings carry several implications for carbon governance. Decarbonization strategies should prioritize structurally central nodes, not just the largest emitters, to achieve systemic leverage. Cross-sectoral coordination and regional cooperation must be embedded in national mitigation planning, particularly within entrenched industrial clusters. Policy design should shift from static targets to flow-oriented interventions, addressing how carbon is transmitted, intermediated, and institutionally reinforced.

Supplementary data

Table A.1| Regions selected in this study

Abbr	Province	Region	Abbr	Province	Region
BJ	Beijing	North China	HA	Henan	Central China
TJ	Tianjin	North China	HB	Hubei	Central China
HE	Hebei	North China	HN	Hunan	Central China
SX	Shanxi	North China	GD	Guangdong	South China
NM	Inner Mongolia	North China	GX	Guangxi	South China
LN	Liaoning	Northeast China	HI	Hainan	South China
JL	Jilin	Northeast China	CQ	Chongqing	Southwest China
HL	Heilongjiang	Northeast China	SC	Sichuan	Southwest China
SH	Shanghai	East China	GZ	Guizhou	Southwest China
JS	Jiangsu	East China	YN	Yunnan	Southwest China
ZJ	Zhejiang	East China	SN	Shaanxi	Northwest China
AH	Anhui	East China	GS	Gansu	Northwest China
FJ	Fujian	East China	QH	Qinghai	Northwest China
JX	Jiangxi	East China	NX	Ningxia	Northwest China
SD	Shandong	East China	XJ	Xinjiang	Northwest China

Table A.2| Sectoral classification from input-output table of China

No	Sector	Industry classification
S1	Farming, Forestry, Animal Husbandry and Fishery	Agriculture
S2	Mining and washing of coal	Energy industry
S3	Extraction of petroleum and natural gas	Energy industry
S4	Mining and processing of metal ores	Energy industry
S5	Mining and processing of nonmetal ores	Energy industry
S6	Manufature of foods and tobacco	Light industry
S7	Manufature of textile	Light industry
S8	Manufacture of textile wearing apparel, footwear, caps, leather, furs, feather (down), and related products	Light industry
S9	Processing of timber, manufacture of furniture	Light industry
S10	Manufacture of paper, printing, Manufacture of articles for culture, education, and sports activities	Light industry
S11	Processing of petroleum, coking, and processing of nuclear fuel	Energy industry
S12	Chemical industry	Heavy industry
S13	Manufacture of non-metallic mineral products	Heavy industry
S14	Smelting and processing of metals	Heavy industry
S15	Manufacture of metal products	Heavy industry
S16	Manufacture of general purpose machinery	Heavy industry
S17	Manufacture of special purpose machinery	Heavy industry
S18	Manufacture of transport equipment	Heavy industry
S19	Manufacture of electrical machinery and equipment	High-tech industry

No	Sector	Industry classification
S20	Manufacture of communication equipment, computers and other electronic equipment	High-tech industry
S21	Manufacture of measuring instruments	High-tech industry
S22	Other manufacturing	High-tech industry
S23	Comprehensive use of waste resources	High-tech industry
S24	Repair of metal products, machinery and equipment	Light industry
S25	Production and distribution of electric power and heat power	Energy industry
S26	Production and distribution of gas	Energy industry
S27	Production and distribution of tap water	Light industry
S28	Construction	Construction
S29	Wholesale and retail trades	Production services
S30	Transport, storage, and postal services	Production services
S31	Hotel and restaurant	Consumer services
S32	Information transfer, software and information technology services	Production services
S33	Finance	Production services
S34	Real estate	Consumer services
S35	Tenancy and commercial services	Production services
S36	Research and experimental development	Production services
S37	Administration of water, environment, and public facilities	Production services
S38	Resident, repair and other services	Consumer services
S39	Education	Consumer services
S40	Health care and social work	Consumer services
S41	Culture, sports, and entertainment	Consumer services
S42	Public administration, social insurance, and social organizations	Consumer services

References

1 Nema, P., Nema, S. & Roy, P. An overview of global climate changing in current scenario and mitigation action. *Renewable and Sustainable Energy Reviews* **16**, 2329-2336 (2012).

2 Tambo, E., Duo-Quan, W. & Zhou, X.-N. Tackling air pollution and extreme climate changes in China: Implementing the Paris climate change agreement. *Environment International* **95**, 152-156 (2016).

3 Teng, F. & Wang, P. The evolution of climate governance in China: drivers, features, and effectiveness. *Environmental Politics* **30**, 141-161 (2021).

4 Xu, G., Dong, H., Xu, Z. & Bhattarai, N. China can reach carbon neutrality before 2050 by improving economic development quality. *Energy* **243**, 123087 (2022).

5 Zhao, X., Ma, X., Chen, B., Shang, Y. & Song, M. Challenges toward carbon neutrality in China: Strategies and countermeasures. *Resources, Conservation and Recycling* **176**, 105959 (2022).

6 Wang, F., Wu, M. & Zheng, W. What are the impacts of the carbon peaking and carbon neutrality target constraints on China?s economy? *Environmental Impact Assessment Review* **101** (2023). https://doi.org/10.1016/j.eiar.2023.107107

7 Chen, H., Qi, S. & Tan, X. Decomposition and prediction of China's carbon emission intensity towards carbon neutrality: from perspectives of national, regional and sectoral level. *Science of The Total Environment* **825**, 153839 (2022).

8 Lin, Z. & Liao, X. Synergistic effect of energy and industrial structures on carbon emissions in China. *Journal of Environmental Management* **345**, 118831 (2023).

9 Lin, B. & Zhao, H. Asymmetric trade barriers and CO2 emissions in carbon-intensive industry. *Journal of Environmental Management* **349**, 119547 (2024).

10 Unruh, G. C. Understanding carbon lock-in. *Energy Policy* **28**, 817-830 (2000). https://doi.org/https://doi.org/10.1016/S0301-4215(00)00070-7

11 Unruh, G. C. Escaping carbon lock-in. *Energy Policy* **30**, 317-325 (2002). https://doi.org/https://doi.org/10.1016/S0301-4215(01)00098-2

12 Tabash, M. I., Farooq, U., El Refae, G. A. & Qasim, A. Exploring the carbon footprints of economic growth, foreign investment, energy dependency and financial development: does EKC work in GCC region? *Management of Environmental Quality: An International Journal* **34**, 273-289 (2022). https://doi.org/10.1108/meq-05-2022-0137

13 Yu, Y., Jian, X., Won, D. & Jahanger, A. Breaking the carbon bind: How digitalization and energy transformation reshape carbon dependency based on wavelet and machine learning approaches. *Environmental Development* **55**, 101226 (2025). https://doi.org/https://doi.org/10.1016/j.envdev.2025.101226

14 Guo, C. *et al.* The unintended dilemma of China's target-based carbon neutrality policy and provincial economic inequality. *Energy Economics* **126**, 107002 (2023).

15 Liu, Z. *et al.* Challenges and opportunities for carbon neutrality in China. *Nature Reviews Earth & Environment* **3**, 141-155 (2022).

16 Jia, L. *et al.* Spatial correlation investigation of carbon emission efficiency in the Yangtze River Delta of China: The role of low-carbon pilot cities. *Ecological Indicators* **172**, 113282 (2025).

17 Mehmood, K., Hassan, S. T., Qiu, X. & Ali, S. Comparative analysis of CO2 emissions and economic performance in the United States and China: Navigating sustainable development in the climate change era. *Geoscience Frontiers* **15**, 101843 (2024).

18 Bandara, P., Ray, R., Lu, J. & Gallagher, K. P. Developing countries locked out of low-carbon technology trade. *Science* **388**, 248-250 (2025).

19 Pan, X., Wang, M. & Li, M. Low-carbon policy and industrial structure upgrading: Based on the perspective of strategic interaction among local governments. *Energy Policy* **183**, 113794 (2023).

20 Zhang, H., Sun, X., Bi, C., Ahmad, M. & Wang, J. Can sustainable development policy reduce carbon emissions? Empirical evidence from resource-based cities in China. *Science of the Total Environment* **838**, 156341 (2022).

21 Liu, J., Wang, K., Zou, J. & Kong, Y. The implications of coal consumption in the power sector for China’s CO2 peaking target. *Applied Energy* **253**, 113518 (2019).

22 Zhang, S. *et al.* Targeting net-zero emissions while advancing other sustainable development goals in China. *Nature Sustainability* **7**, 1107-1119 (2024).

23 Xian, B., Xu, Y., Chen, W., Wang, Y. & Qiu, L. Co-benefits of policies to reduce air pollution and carbon emissions in China. *Environmental Impact Assessment Review* **104**, 107301 (2024).

24 Shen, R. *et al.* Research on carbon compensation zoning guided by major function zones: A case study of the Yangtze River Delta region. *Ecological Indicators* **173**, 113383 (2025).

25 Bai, L. *et al.* Effects of digital economy on carbon emission intensity in Chinese cities: A life-cycle theory and the application of non-linear spatial panel smooth transition threshold model. *Energy Policy* **183**, 113792 (2023).

26 Zhang, W. *et al.* The economy–employment–environmental health transfer and embedded inequities of China's capital metropolitan area: a mixed-methods study. *The Lancet Planetary Health* **7**, e912-e924 (2023).

27 Tian, P. *et al.* Water-energy-carbon nexus in China's intra and inter-regional trade. *Science of the Total Environment* **806**, 150666 (2022).

28 Fu, W., Yang, S., Hu, S. & Zhang, P. The impact of embodied land flow in interregional trade on carbon emissions in China. *Applied Geography* **159**, 103065 (2023).

29 Ju, H., Zeng, G. & Zhang, S. Inter-provincial flow and influencing factors of agricultural carbon footprint in China and its policy implication. *Environmental Impact Assessment Review* **105** (2024). https://doi.org/10.1016/j.eiar.2024.107419

30 Xu, C., Zhu, Q., Li, X., Wu, L. & Deng, P. Determinants of global carbon emission and aggregate carbon intensity: A multi-region input− output approach. *Economic Analysis and Policy* **81**, 418-435 (2024).

31 Shi, C. *et al.* Unveiling the unequal variation of regional carbon risk under inter-provincial trade in China. *Environmental Impact Assessment Review* **105** (2024). https://doi.org/10.1016/j.eiar.2023.107391

32 Guo, S., Zhao, Q., He, P., Wang, Y. & Zhang, X. Embodied black carbon emission transfer within and across the Jing-Jin-Ji urban agglomeration. *Environmental Impact Assessment Review* **110**, 107678 (2025).

33 Wang, Y. *et al.* Exploring the path of inter-provincial industrial transfer and carbon transfer in China via combination of multi-regional input–output and geographically weighted regression model. *Ecol. Indic* **125**, 10.1016 (2021).

34 Wang, Q., Yang, X. & Li, R. Are low-carbon emissions in the South at the cost of high-carbon emissions in North China? A novel assessment. *Environmental Impact Assessment Review* **105** (2024). https://doi.org/10.1016/j.eiar.2024.107426

35 Tao, T. & Wen, G. Research on accounting of provincial carbon transfer: based on the empirical data of 30 provinces in China. *Environmental Science and Pollution Research* **29**, 40984-40996 (2022).

36 Zheng, H. *et al.* Regional determinants of China's consumption-based emissions in the economic transition. *Environmental Research Letters* **15**, 074001 (2020).

37 Wang, Q. & Han, X. Is decoupling embodied carbon emissions from economic output in Sino-US trade possible? *Technological Forecasting and Social Change* **169**, 120805 (2021).

38 Li, Y., Chen, B. & Chen, G. Carbon network embodied in international trade: global structural evolution and its policy implications. *Energy Policy* **139**, 111316 (2020).

39 Wang, S., Wang, X. & Chen, S. Global value chains and carbon emission reduction in developing countries: does industrial upgrading matter? *Environmental Impact Assessment Review* **97**, 106895 (2022).

40 Chen, M. & Xu, Z. Assessing socio-ecological fit of international environmental agreements and trade-embodied carbon flows. *Environmental Impact Assessment Review* **106** (2024). https://doi.org/10.1016/j.eiar.2024.107534

41 Han, M., Yao, Q., Lao, J., Tang, Z. & Liu, W. China's intra-and inter-national carbon emission

transfers by province: A nested network perspective. *Science China Earth Sciences* **63**, 852-864 (2020).

42 Wang, G., Wang, Y., Liu, K. & Sun, S. A classification and recognition algorithm of key figures in public opinion integrating multidimensional similarity and K-shell based on supernetwork. *Humanities and Social Sciences Communications* **11**, 1-19 (2024).

43 Gidel, G., Berard, H., Vignoud, G., Vincent, P. & Lacoste-Julien, S. A variational inequality perspective on generative adversarial networks. *arXiv preprint arXiv:1802.10551* (2018).

44 Shengjiu, L., Tianrui, L., Jia, L. & Peng, X. Research on multi-fractals of weighted hypernetworks. *JUSTC* **50**, 369-381 (2020).

45 Liu, Z., Chen, W., Zhang, C., Yang, C. & Cheng, Q. Intelligent scheduling of a feature-process-machine tool supernetwork based on digital twin workshop. *Journal of manufacturing systems* **58**, 157-167 (2021).

46 Sun, Y., Wang, P., Wang, Y. & Wang, Z. Dynamic Information Propagation Model of Social Hypernetwork Considering Positive and Negative Interference. (2023).

47 Fu, R., Qiang, Q. P., Ke, K. & Huang, Z. Closed-loop supply chain network with interaction of forward and reverse logistics. *Sustainable Production and Consumption* **27**, 737-752 (2021).

48 Yinghua, S., Mingxuan, B., Yaping, M. & Feizhou, H. Super-network model of emergency resource scheduling considering multi-agent psychological effect. *China Safety Science Journal* **31**, 158 (2021).

49 Zhou, L., Li, F., Gong, Y. & Hu, F. Identification methods of vital nodes based on k-shell in hypernetworks. *Complex Syst Complex Sci* **18**, 15-22 (2021).

50 Dong, X., Lian, Y., Chi, Y., Tang, X. & Liu, Y. A two-step rumor detection model based on the supernetwork theory about Weibo. *The Journal of Supercomputing* **77**, 12050-12074 (2021).

51 Wenwei, G., Xianchun, L., Xuechun, Z. & Jingxian, C. Product quality control strategy based on supply chain network equilibrium in the direct broadcasting economy. *Computer Integrated Manufacturing System* **29**, 1684 (2023).

52 Duan, C. *et al.* Interregional carbon flows of China. *Applied Energy* **227**, 342-352 (2018).

53 Sun, L. *et al.* Analyzing carbon emission transfer network structure among provinces in China: new evidence from social network analysis. *Environmental Science and Pollution Research* **27**, 23281-23300 (2020).

54 Sun, Y.-Y., Faturay, F., Lenzen, M., Gössling, S. & Higham, J. Drivers of global tourism carbon emissions. *Nature Communications* **15**, 1-10 (2024).

55 Shan, Y. *et al.* China CO2 emission accounts 1997–2015. *Scientific data* **5**, 1-14 (2018).

56 Shan, Y., Huang, Q., Guan, D. & Hubacek, K. China CO2 emission accounts 2016–2017. *Scientific data* **7**, 54 (2020).

57 Chi, Y., Tang, X., Lian, Y., Dong, X. & Liu, Y. A supernetwork-based online post informative quality evaluation model. *Knowledge-Based Systems* **168**, 10-24 (2019).

58 Liao, F., Arentze, T. & Timmermans, H. Multi-state supernetwork framework for the two-person joint travel problem. *Transportation* **40**, 813-826 (2013).

59 Yuxi, Z., Jingke, H., Wen, Q., Yang, C. & Danfei, N. Managing water-land-food nexus towards resource efficiency improvement: A superedge-based analysis of China. *Journal of Environmental Management* **325**, 116607 (2023). https://doi.org/https://doi.org/10.1016/j.jenvman.2022.116607

60 Yuxi, Z., Jingke, H., Chenyang, S., Jiexu, Y. & Shihan, Z. Heterogeneous interactions in the

water-land-food nexus in shaping resource efficiency: A supernetwork simulation. *Sustainable Production and Consumption* **40**, 63-75 (2023).

61 Yuxi, Z., Jingke, H., Changlin, X. & Zhangmiao, L. Unfolding the synergy and interaction of water-land-food nexus for sustainable resource management: A supernetwork analysis. *Science of The Total Environment* **784**, 147085 (2021). https://doi.org/https://doi.org/10.1016/j.scitotenv.2021.147085

62 Han, S., Pool, J., Tran, J. & Dally, W. Learning both weights and connections for efficient neural network. *Advances in neural information processing systems* **28** (2015).

63 Liang, T., Glossner, J., Wang, L., Shi, S. & Zhang, X. Pruning and quantization for deep neural network acceleration: A survey. *Neurocomputing* **461**, 370-403 (2021).

64 Lei, W., Chen, H. & Wu, Y. in *Proceedings of the 2nd International Conference on Intelligent Information Processing.* 1-6.

65 Barrat, A., Barthelemy, M., Pastor-Satorras, R. & Vespignani, A. The architecture of complex weighted networks. *Proceedings of the national academy of sciences* **101**, 3747-3752 (2004).

66 Freeman, L. C. A set of measures of centrality based on betweenness. *Sociometry*, 35-41 (1977).

67 Freeman, L. C. Centrality in social networks: Conceptual clarification. *Social network: critical concepts in sociology. Londres: Routledge* **1**, 238-263 (2002).

68 Hu, F., Zhao, H. & Ma, X. An evolving hypernetwork model and its properties. *Scientia Sinica Physica, Mechanica & Astronomica* **43**, 16 (2013).

69 Seidman, S. B. Network structure and minimum degree. *Social networks* **5**, 269-287 (1983).

70 Dorogovtsev, S. N., Goltsev, A. V. & Mendes, J. F. F. K-core organization of complex networks. *Physical review letters* **96**, 040601 (2006).

71 Zhao, B., Chen, X. & Zhang, J. Cycle degree of an industry and its algorithm. *Systems Engineering-Theory & Practice* **34**, 1388-1397 (2014).

72 Friedkin, N. E. The development of structure in random networks: an analysis of the effects of increasing network density on five measures of structure. *Social Networks* **3**, 41-52 (1981).

73 Shan, Y. *et al.* China CO2 emission accounts 1997–2015. *Scientific Data* **5**, 170201 (2018). https://doi.org/10.1038/sdata.2017.201

74 Feng, C., Yang, L., Luo, M. & Liu, Q. A framework of payments for water-related ecosystem services (PWES) based on green water management. *Journal of Cleaner Production* **425**, 138930 (2023). https://doi.org/https://doi.org/10.1016/j.jclepro.2023.138930

75 Frölicher, T. L. Strong warming at high emissions. *Nature Climate Change* **6**, 823-824 (2016). https://doi.org/10.1038/nclimate3053

76 Wang, T., Teng, F., Deng, X. & Xie, J. Climate module disparities explain inconsistent estimates of the social cost of carbon in integrated assessment models. *One Earth* **5**, 767-778 (2022). https://doi.org/10.1016/j.oneear.2022.06.005

77 Trencher, G., Rinscheid, A., Duygan, M., Truong, N. & Asuka, J. Revisiting carbon lock-in in energy systems: Explaining the perpetuation of coal power in Japan. *Energy Research & Social Science* **69**, 101770 (2020). https://doi.org/https://doi.org/10.1016/j.erss.2020.101770